MICROSTRUCTURE AND MECHANICAL PROPERTIES OF Fe-Al-Si ALLOYS

HAUŠILD Petr[1]*, ČECH Jaroslav[1], KARLÍK Miroslav[1], PRŮŠA Filip[2], NOVÁK Pavel[2], KOPEČEK Jaromír[3]

[1]*Czech Technical University in Prague, Faculty of Nuclear Sciences and Physical Engineering, Department of Materials, Prague, Czech Republic, EU, * petr.hausild@fjfi.cvut.cz*
[2]*University of Chemistry and Technology Prague, Department of Metals and Corrosion Engineering, Prague, Czech Republic, EU*
[3]*Institute of Physics, ASCR, v.v.i., Department of Functional Materials, Prague, Czech Republic, EU*

Abstract

In this work, the effect of processing conditions on microstructure and mechanical properties of Fe-Al-Si alloys is studied. The microstructure and mechanical properties during each step of processing consisting of mechanical alloying and spark plasma sintering are characterized by means of light microscopy, scanning electron microscopy, x-ray diffraction and micro/nano hardness measurements. Effect of mechanical alloying conditions (especially milling time) on chemical/phase composition, microstructure and overall mechanical properties of spark plasma sintered samples is presented and discussed.

Keywords: Powder metallurgy, mechanical alloying, spark plasma sintering, iron aluminide, iron silicide

1. INTRODUCTION

Increasing need for conserving the strategic elements such as chromium and nickel impels the steel-makers to search for an alternative to chromium-alloyed stainless and heat-resistant steels as well as nickel-based alloys for corrosive environments and high-temperature applications. Among currently investigated materials, the iron-based intermetallics are the most promising materials [1 - 3]. Ternary Fe-Al-Si alloys show quite unique properties e.g. excellent corrosion properties in oxidizing and sulfidizing environment, high-temperature oxidation resistance and wear resistance [4]. However, these alloys exhibit difficulties with conventional routes of processing such as casting and hot and/or cold rolling.

Another way of processing could be mechanical alloying (MA) which is a powder processing technique that allows production of homogeneous materials starting from blended elemental powder mixtures [5]. Mechanical alloying involves the severe deformation, repeated cold welding, fracturing and rewelding of a mixture of powder particles in a high-energy ball charge. Such an alloy can then be created without melting, the intense deformation associated with mechanical alloying can force atoms into positions where they may not prefer to be at equilibrium; i.e. the alloy is in a mechanically homogenized non-equilibrium state (mechanical mixture). Mechanical alloying allows produce a controlled, extremely fine microstructure. However, subsequent sintering of powders at high temperature and long annealing time can lead to the coarsening or even to alloy decomposition into thermodynamically more stable phases [6].

For this reason, it is convenient using of spark plasma sintering (SPS) [7, 8]. In this method, the powder is placed between two punches being also two electrodes. Then, high amperage electric current (pulse or direct) is passed through the powder seated in the die which is also simultaneously pressed. The powder is heated by the electric current and subjected to the pressure. Several unique parameters of this method can be reported. Foremost, the very high heating rates, much higher than that of e.g. hot isostatic pressing, can be achieved. This leads to high rates of densification whereas the coarsening process is suppressed. Due to the short processing time resulting in minimal grain growth of consolidated materials, the method can also be used for nano-sized powders [7].

In this work, the effect of processing conditions on microstructure and mechanical properties of Fe-Al-Si alloys is presented and discussed. The microstructure and mechanical properties during each step of processing consisting of mechanical alloying and spark plasma sintering are characterized by means of light microscopy, scanning electron microscopy (SEM), X-ray diffraction (XRD) and micro/nano hardness measurements.

2. EXPERIMENTAL DETAILS

2.1. Mechanical alloying

Composition of the alloy was chosen FeAl20Si20 (wt.%) in order to compare the microstructure and properties with alloy previously prepared by reactive sintering [9]. The feedstock material for mechanical alloying consisted of Al (Strem Chemicals, purity of 99.7 %), Si (Alfa Aesar, purity of 99.5 %) and Fe (Strem Chemicals, purity of 99.9 %) powders, which contained powder particles with average dimensions of 44 μm (Al and Si) and 9 μm (Fe), respectively. Powders were blended in appropriate amounts to form 5 g batch mixture which was afterwards placed into a steel mould (Retsch PM 100) together with milling balls. Both steel mould and milling balls were made from AISI 420 stainless steel. The mould was sealed and flushed for at least 5 min with argon to prevent undesirable oxidation during the mechanical alloying. The powder to ball mass ratio was set to be 1:15, rotational speed was 400 rpm. The total duration of the process varied from 0.5 to 24 hours. During the process, small amounts of mechanically alloyed powders were collected for metallographic and XRD analyses in order to determine the present phases and to describe the evolution of phase compositions as a function of the total time of the MA.

2.2. Spark plasma sintering

The powder was sintered using a FCT Systeme HP D10 device. The tool system placed inside the vacuum chamber consists of a graphite punch-and-die unit where the powders are loaded. Both punches are connected via graphite protection plates to electrodes. To prevent sticking between the loose powder and the graphite parts, these are interspaced by graphite paper. The temperature of the compacting unit is measured by a pyrometer located above the punch-and-die unit. The pyrometer is focused on the bottom of a hole going through the piston, protection plate and part of the upper punch. An extensive description of the equipment is given elsewhere [10].

Disc specimens having 20 mm in diameter and height of approximately 8 mm were sintered at 1000 °C. During the process, the sample was heated by direct current (DC) at a heating rate of 300 °C/min up to 900 °C with subsequent heating rate 100 °C/min up to 1000 °C to minimize the sintering temperature overshoot. After reaching the temperature 1000 °C, the sample was compressed by a pressure of 50 MPa. The total time the sample remained at 1000 °C was 10 minutes after which a slow cooling step with a cooling speed of 50 °C/min was set with simultaneous compaction pressure reduction till the sample reached temperature of 300 °C.

2.3. Characterization techniques

Microstructure of powders was characterized after various durations of mechanical alloying as well as after final spark plasma sintering. Individual particles of powders after various durations of mechanical alloying were embedded in the conductive resin and metallographically polished with final step in 0.04 μm colloidal silica suspension (OPS). Samples from SPS sinters were cut by low-speed diamond saw in the central part of the sintered cylinders and metallographically polished by standard procedure.

Microstructural observations were carried out by means of the metallographic microscope Neophot 32 and Jeol JSM 5510LV scanning electron microscope equipped with iXRF 5000 energy dispersive X-ray spectroscopy analyzer. Phase composition was determined by a PANalytical X'Pert Pro X-ray diffractometer with Cu K_α cathode (λ = 1.54059·10^{-10} m) in Bragg-Brentano geometry. Nanoindentation measurements were performed on Anton Paar NHT Nanoindentation Tester with Berkovich indenter using instrumented indentation

technique [11, 12]. The results were evaluated according to the ISO 14577 standard [13]. Based on preliminary experiments, the load of 5 mN was chosen in order to be able to compare the hardness of individual mechanically alloyed powders (not affected by embedding resin) with the hardness of sintered samples. At least ten indentations were carried out (in the case of embedded powders in ten different particles) in order to assure the statistically representative results.

3. RESULTS

3.1. Mechanical alloying

Microstructure of powders (**Figure 1**) was characterized after 0 h; 0.5 h; 1 h; 2 h; 3 h; 4 h; 6 h; 8 h; 10 h and 24 h of milling (mechanical alloying). At the first stage of milling (during the rapid fracturing and cold welding), convoluted lamellae can be observed within the particles. With increasing time of milling, lamellae get finer and more convoluted along with the beginning of dissolution (**Figure 2**). Almost complete solid solution formation was observed after 4 h of milling. Energy dispersive X-ray spectroscopy revealed that extensive increasing of milling time (i.e. 24 h) led to contamination of powders by chromium probably from the milling vessel.

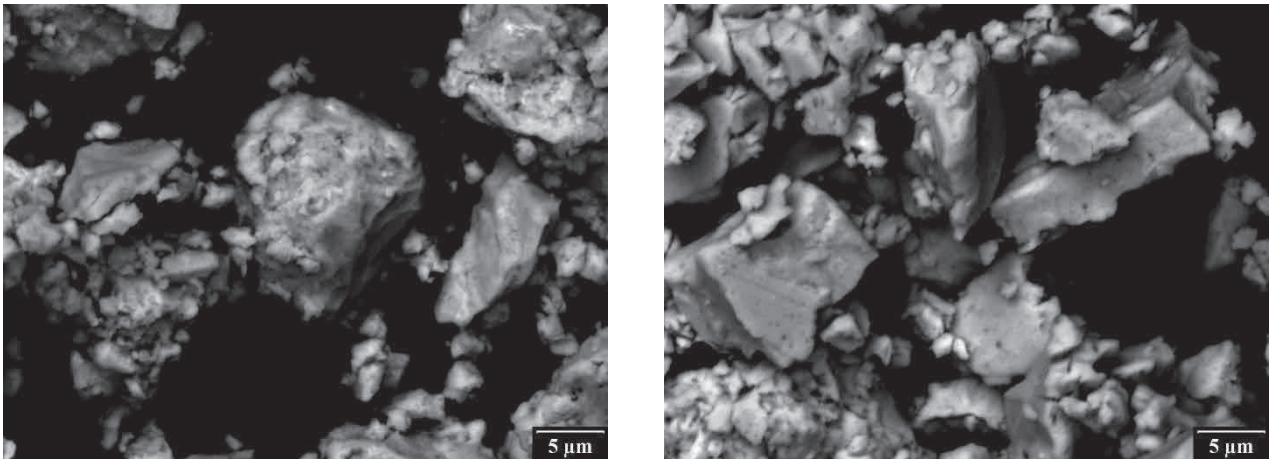

3 h at 400 rpm 24 h at 400 rpm

Figure 1 Particles after milling 5 g of elemental powders at 400 rpm (SEM, back-scattered electron signal)

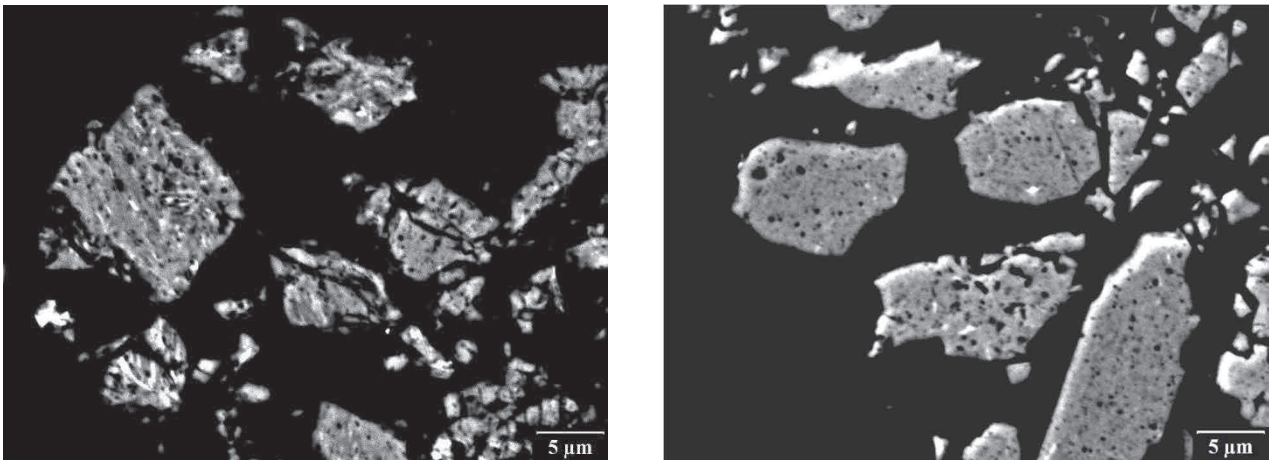

3 h at 400 rpm 24 h at 400 rpm

Figure 2 Microstructure of individual particles after milling of elemental powders at 400 rpm for different time (SEM, back-scattered electron signal)

X-ray diffraction unambiguously detected peaks corresponding to intermetallic phases after 2 h of milling. With increasing time of milling (see **Figure 3**), the amount of intermetallic phases gradually increased until the phase composition reached a mixture of Fe_3Si and FeSi (supersaturated by Al due to mechanical alloying). Mechanical alloying led to peak shift and peak broadening, which can be attributed partly to the formation of supersaturated solid solution, significant grain refinement and the change in the lattice parameters induced by extensive deformation during MA.

Nanohardness of particles after milling showed firstly an increasing trend with the milling time (H_{IT} increased from H_{IT} = 10.2 ± 2.3 GPa after 1 h of milling to H_{IT} = 15.8 ± 2.1 GPa after 4 h of milling) then it showed slight decrease (to H_{IT} = 13.4 ± 2.7 GPa after 24 h of milling) which could probably be associated with the contamination of powders by chromium leading to the solid solution softening.

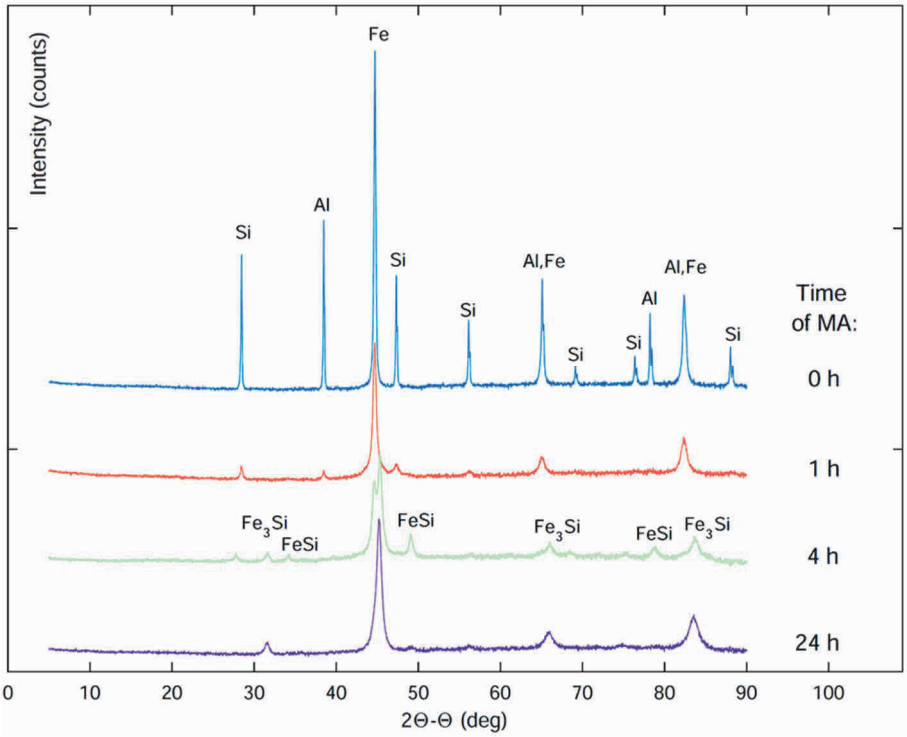

Figure 3 XRD patterns of mechanically alloyed powders after different time of milling at 400 rpm

3.2. Spark plasma sintering

Based on the previous results obtained on mechanically alloyed powders after different time of milling, optimum condition of MA for spark plasma sintering were chosen, i.e. powders milled 4 h at 400 rpm. Microstructure of such spark plasma sintered samples is shown in **Figure 4**. Energy dispersive X-ray spectroscopy revealed only areas with chemical composition close to the nominal (FeAl20Si20 wt.%). Local variations in chemical composition can be attributed to the presence of intermetallic phases after milling (as detected by XRD). No traces of initial pure powders were found in spark plasma sintered samples.

Measured nanohardness of SPS samples from powders milled 4 h was in a good agreement with hardness of milled powders (H_{IT} = 15.1±1.7 GPa for SPS samples comparing to H_{IT} = 15.8±2.1 GPa of 4 h milled powders), which means that mechanical properties were not significantly affected by pre-heating and heating during spark plasma sintering.

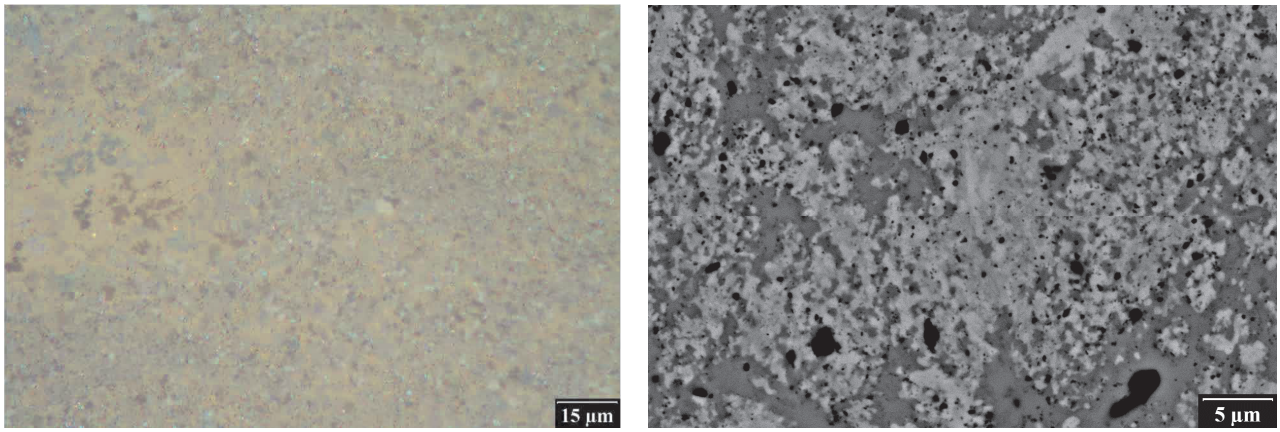

Figure 4 Microstructure of spark plasma sintered samples from powders milled 4 h at 400 rpm (left - light microscopy, right - SEM, back-scattered electron signal)

4. CONCLUSIONS

The effect of processing conditions on microstructure and mechanical properties of Fe20Al20Si (wt.%) alloys was examined.

The microstructure and mechanical properties during each step of processing consisting of mechanical alloying and spark plasma sintering were characterized by:

- light microscopy,
- scanning electron microscopy,
- energy dispersive X-ray spectroscopy,
- X-ray diffraction,
- nanoindentation.

Optimum conditions of mechanical alloying (4 h milling at 400 rpm) were used for spark plasma sintering.

Correctly spark plasma sintered samples (10 min at 1000 ºC/50 MPa) preserved phase composition and mechanical properties of milled powders.

ACKNOWLEDGEMENTS

This research was carried out in the frame of projects 17-07559S (Czech Science Foundation) and SGS16/172/OHK4/2T/14 (Czech Technical University in Prague).

REFERENCES

[1] STOLOFF, N. S., SIKKA, V. K. *Physical Metallurgy and processing of Intermetallic Compounds. 1st ed.* New York. Chapman & Hall, 1996, 684 p.

[2] KRATOCHVÍL, P. The history of the search and use of heat resistant Pyroferal© alloys based on FeAl. *Intermetallics,* 2008, vol. 16, no. 4, pp. 587-591.

[3] KRATOCHVÍL, P., KARLÍK, M., HAUŠILD, P., CIESLAR, M. Influence of annealing on mechanical properties of an Fe-28Al-4Cr-0.1Ce alloy. *Intermetallics,* 1999, vol. 7, no. 7, pp. 847-853.

[4] NOVÁK, P., ZELINKOVÁ, M., ŠERÁK, J., MICHALCOVÁ, A., NOVÁK, M., VOJTĚCH, D. Oxidation resistance of SHS Fe-Al-Si alloys at 800 °C in air. *Intermetallics* 2011, vol. 19, no. 9, pp. 1306-1312.

[5] SURYANARAYANA C. Mechanical alloying and milling. *Progress in Materials Science*. 2001, vol. 46, pp. 1-184.

[6] BHADESHIA, H. K. D. H. Mechanically Alloyed Metals. *Materials Science and Technology*, 2000, vol. 16, pp. 1404-1411.

[7] ORRÙ, R., LICHERI, R. LOCCI, A. M., CINCOTTI, A., CAO, G. Consolidation/synthesis of materials by electric current activated/assisted sintering. *Materials Science and Engineering R*, 2009, vol. 63, pp. 127-287.

[8] SKIBA, T., HAUŠILD, P., KARLÍK, M., VANMEENSEL, K., VLEUGELS J. Mechanical properties of spark plasma sintered FeAl intermetallics. *Intermetallics*, 2010, vol. 18, no. 7, pp. 1410-1414.

[9] NOVÁK, P., KNOTEK, V., ŠERÁK, J., MICHALCOVÁ, A., VOJTĚCH, D. Synthesis of Fe-Al-Si intermediary phases by reactive sintering. *Powder Metallurgy*, 2011, vol. 54, no. 2, pp. 167-171.

[10] GUILLON, O., GONZALEZ-JULIAN, J., DARGATZ, B., KESSEL, T., SCHIERNING, G., RÄTHEL, J., HERRMANN, M. Field-Assisted Sintering Technology/Spark Plasma Sintering: Mechanisms, Materials, and Technology Developments, *Advanced Engineering Materials*, 2014, vol. 16, no. 7, pp. 830-849.

[11] OLIVER, W.C., PHARR, G.M. An Improved Technique for Determining Hardness and Elastic Modulus using Load and Displacement Sensing Indentation Experiments. *Journal of Materials Research,* Vol. 7, No. 6, 1992, pp. 1564-1583.

[12] OLIVER, W.C., PHARR, G.M. Measurement of hardness and elastic modulus by instrumented indentation, Advances in understanding and refinements to methodology. *Journal of Materials Research,* Vol. 19, No. 1, 2004, pp. 3-20.

[13] ISO 14577-1:2015, *Instrumented indentation test for hardness and materials parameters - Part 1: Test method*. ISO Standard. 2015.